Neuropharmacology 177 (2020) 108257

Contents lists available at ScienceDirect

Neuropharmacology

journal homepage: www.elsevier.com/locate/neuropharm

Invited Review

Nicotinic receptor pharmacology *in silico*: Insights and challenges

Alican Gulsevin

Department of Chemistry, Vanderbilt University, Nashville, TN, USA, 37221

ARTICLE INFO

Keywords:
Ligand-gated ion channel
Nicotinic acetylcholine receptor
α7 nAChR
Structure modeling
Allosteric activation
Computational modeling

ABSTRACT

Nicotinic acetylcholine receptors (nAChR) are homo- or hetero-pentameric ligand-gated ion channels of the Cys-loop superfamily and play important roles in the nervous system and muscles. Studies on nAChR benefit from *in silico* modeling due to the lack of high-resolution structures for most receptor subtypes and challenges in experiments addressing the complex mechanism of activation involving allosteric sites. Although there is myriad of computational modeling studies on nAChR, the multitude of the methods and parameters used in these studies makes modeling nAChR a daunting task, particularly for the non-experts in the field. To address this problem, the modeling literature on *Torpedo* nAChR and α7 nAChR were focused on as examples of heteromeric and homomeric nAChR, and the key *in silico* modeling studies between the years 1995–2019 were concisely reviewed. This was followed by a critical analysis of these studies by comparing the findings with each other and with the emerging experimental and computational data on nAChR. Based on these critical analyses, suggestions were made to guide the future researchers in the field of *in silico* modeling of nAChR.

This article is part of the special issue on 'Contemporary Advances in Nicotine Neuropharmacology'.

1. Introduction

Nicotinic acetylcholine receptors (nAChR) are pentameric ligand-gated ion channels that are members of the Cys-loop superfamily (Changeux, 2012). Each nAChR pentamer consists of an extracellular domain (ECD) that plays a role in ligand binding, a transmembrane domain (TMD) with a central ion channel, and an intracellular domain (ICD) (Fig. 1). Traditional agonists and antagonists of nAChR bind to orthosteric sites on the ECD. Heteromeric nAChR have two orthosteric sites between neighboring α and non-α subunits of the receptor (Blount and Merlie, 1989), whereas homomeric nAChR have five potential binding sites (Elgoyhen et al., 1994; Palma et al., 1996). The TMD of each nAChR subunit consists of four helices M1-M4. The ion pore is lined by the M2 helices of the five subunits (Hucho et al., 1986), and the short M2-M3 linker interacts with the ECD (Bertrand et al., 2008). The disordered M3-M4 loop is also known as the ICD, which shows great variability among nAChR subtypes and is considered to play a role in interactions with other cellular proteins (Stokes et al., 2015). Finally, the M4 helix is considered to play a role in protein folding and modulation of membrane-α7 interactions (Hénault et al., 2015).

Muscle-type *Torpedo* nAChR (Unwin, 2005; Unwin and Fujiyoshi, 2012), and more recently, α4β2 nAChR (Morales-Perez et al., 2016; Walsh et al., 2018) and α3β4 structures (Gharpure et al., 2019) including both the ECD and the TMD domains (ECD/TMD) are available in the Protein Data Bank at ~ 3–4 Å resolution. However, structural data on the remaining nAChR are fragmentary. The nAChR subunit structures solved so far include the ECD of monomeric nAChR subunits α1 (Dellisanti et al., 2007; Noridomi et al., 2017), α2 (Kouvatsos et al., 2016), α9 (Zouridakis et al., 2019, 2014), and the solution NMR structure of the α7 TMD (Mowrey et al., 2013).

In this work, key studies on *in silico* modeling of nAChR were reviewed with a particular focus on the muscle-type *Torpedo* nAChR and α7 nAChR with the aim to provide a holistic picture of our current understanding of heteromeric and homomeric nAChR mode of action and the state of the art in computational modeling of nAChR, specifically focused on α7 nAChR. In order to keep the review fluent and focused, discussion of particular experimental details was avoided, but the interested reader can find information regarding the simulation times, membrane models used in simulations, templates used for homology modeling and their references in Supporting Table 1 Also, canonical mature α7 numbering [https://www.ncbi.nlm.nih.gov/nuccore/NM_000746.6] and M2 helix residue numbering proposed by Miller (1989) were used instead of the arbitrary numbering used in some studies to prevent confusion and inconsistencies.

2. Experimental and computational studies with *Torpedo* nAChR

Our original understanding on the structure and mechanism of nAChR comes from mutation and labeling experiments with the *Torpedo*

E-mail address: alican.gulsevin@vanderbilt.edu.

https://doi.org/10.1016/j.neuropharm.2020.108257
Received 15 January 2020; Received in revised form 16 July 2020; Accepted 26 July 2020
Available online 29 July 2020

Abbreviations

nAChR	nicotinic acetylcholine receptor
ACh	acetylcholine
ECD	extracellular domain
TMD	transmembrane domain
ICD	intracellular domain
MD	molecular dynamics
RAMD	random accelerated molecular dynamics
SMD	steered molecular dynamics
Ta-MD	temperature-accelerated molecular dynamics
NMA	normal mode analysis
FRODA	framework rigidity optimized dynamics algorithm
AChBP	acetylcholine binding protein
α7-AChBP	humanized chimeric acetylcholine binding protein
PCA	principal component analysis
RMSD	root mean square deviation
PMF	potential of mean force
MMPBSA	Molecular Mechanics Poisson-Boltzmann Surface Area
MMGBSA	Molecular Mechanics Generalized Born Surface Area
PAM	positive allosteric modulator
ago-PAM	agonist-positive allosteric modulator
DAA	direct allosteric activation
diEPP	diethylphenylpiperazine

nAChR. Prior to the high-resolution *Torpedo* nAChR structures, lower resolution cryo-EM models and photolabeling experiments were used to map the pore-lining M2 helix of the nicotinic receptors. Among these residues was L9′ on the M2 helix facing the channel vestibule, which was hypothesized to play a role as a gatekeeper for ion passage (Yamodo et al., 2010). Mutation of this residue to polar residues were shown to slow desensitization in α7 nAChR and *Torpedo* nAChR (Filatov and White, 1995; Labarca et al., 1995; Revah et al., 1991) and change the mode of action of certain ligands (Palma et al., 1997). Other M2 residues including 1′, 2′, 6′, and 10’ (Chiara et al., 2009; Cohen et al., 1992; Furois-Corbin and Pullman, 1991) were implicated in ion selectivity of the receptor channel.

The M3 domain was also shown to have an α-helical structure based on photolabeling experiments in contact with the remaining TMD helices and to some extent with the membrane (Hamouda et al., 2006; Lugovskoy et al., 1999). The M4 domain is also α-helical and is mostly in contact with the lipid molecules. This domain plays a role in protein folding, expression, and assembly. Mutants of this domain have diminished expression, assembly, or activity (Baenziger et al., 2015; Hamouda et al., 2006; Tamamizu et al., 2000).

Although mutation and photolabeling experiments can give information about the residues important for receptor action, they may not give information about the dynamics of the system. In the absence of reliable experimental methods, computational methods can be used for such analyses. Two methods commonly used to analyze structural changes of proteins are molecular dynamics and normal mode analysis calculations.

Molecular dynamics (MD) simulations are based on simplistic assumptions whereby atoms are modeled as charged spheres, bonded terms are simple linear equations and nonbonded interactions are modeled as pairwise additive terms (Adcock and McCammon, 2006). Despite the simplistic nature MD simulations have been used to sample protein dynamics and ligand-protein interactions for years with success (Mortier et al., 2015). The time scales of the computationally intensive MD simulations are likely to be significantly lower than the physiological timescale of nAChR function (nanosecond to microsecond versus millisecond to second). In fact, most studies surveyed in this work have simulation times below 100 ns, and even longer studies utilize parallel

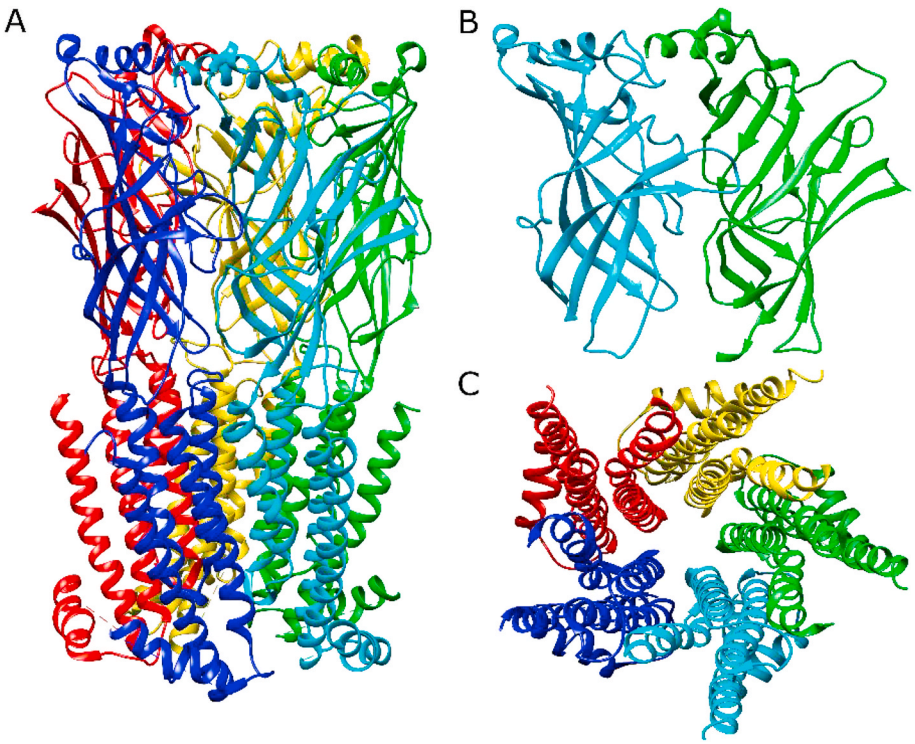

Fig. 1. Structural domains of the nicotinic acetylcholine receptors shown on α4β2 nAChR crystal structure (PDB ID: 5KXI). A) ECD/TMD structure, B) Neighboring two subunits of the ECD, C) Pentameric TMD viewed through the pore axis.

sampling (e.g. multiple short trajectories) to sample the conformational space of the nAChR systems (Supporting Table 1). As a result, methods that rely on application of external potential or force were used in some studies to accelerate the sampling of receptor dynamics or ligand dissociation in a shorter timescale. Random accelerated molecular dynamics (RAMD) (Lüdemann et al., 2000), steered molecular dynamics (SMD) (Grubmüller et al., 1996; Izrailev et al., 1999, 1997), and umbrella sampling (Kästner, 2011; Torrie and Valleau, 1977) are examples to these methods. In a similar manner, targeted molecular dynamics (Ta-MD) (Schlitter et al., 1993) can be used to drive a system into a target conformation within a short amount of time.

An alternative to MD simulations is normal mode analysis (NMA) calculations. NMA calculations utilize a simplified representation of the vibrations in the protein system, which can be used to calculate the effect of local movements on other regions of the protein within a much shorter amount of time than MD simulations (Brooks and Karplus, 1985; Levitt et al., 1985). NMA calculations have been successfully used to identify correlated motions between the protein domains (Bahar et al., 2010; Ma, 2005). Both MD and NMA simulations were used extensively to model the dynamics of nAChR and the mechanism of channel opening.

The general channel activation mechanism proposed for the nAChR involves a quaternary twist that rearranges the positions of the Cys-, β8-β9, and β1-β2 loops at the ECD, which triggers movement of the M2-M3 linker and the pore-lining residues of the M2 helices (Bouzat et al., 2004; Cecchini and Changeux, 2014). Early calculations with the *Torpedo* nAChR structure showed different results regarding the channel activation mechanism based on the computational method of selection. Implicit-membrane MD simulations and NMA calculations with the nAChR TMD with restrained M1, M3, and M4 loops showed kinking of the M2 helix and narrowing of the ion pore around the residues L9′ and L13' in an asymmetric manner, which was interpreted by the authors as a sequential channel gating mechanism (Hung et al., 2005). On the other hand, explicit-membrane MD simulations with the nAChR TMD showed a pore breathing motion of the ion channel defined by the asymmetrical translational motion of the helices M1-M3 followed by a reversion after 30 ns (Xu et al., 2005). However, the pore breathing motion was absent in later NMA calculations with the antagonist α-bungarotoxin-bound nAChR (Samson and Levitt, 2008).

Changes in the orthosteric site and the C-loop were also investigated in computational studies. Early quantum mechanical calculations with nAChR to understand the ligand interactions at the orthosteric site showed that aromatic residues in the orthosteric site form important π-cation interactions with the charged nitrogen of nAChR ligands (Schmitt et al., 1999; Zhong et al., 1998). MD simulations with *Torpedo* nAChR ECD/TMD models showed that C-loop closure triggers upward motion of the β9 and β10 strands, which in turn caused counterclockwise rotation of the M1 and M2 helices around the pore axis (Liu et al., 2008). These structural changes were confirmed by Framework Rigidity Optimized Dynamics Algorithm (FRODA) calculations (Wells et al., 2005) that is based on constrained minimization of the protein structures with the putative closed state of the *Torpedo* nAChR, which identified the C-loop, β2-β3 loop, and the β8-β9 loop as high-mobility regions and the β1-β2 loop and the Cys-loop as moderate-mobility regions (Belfield et al., 2014).

Overall, the calculations with the *Torpedo* nAChR showed mixed results depending on the selected method. Further, it is important to note that the ECD/TMD *Torpedo* nAChR structure used for these simulations (PDB ID: 2BG9) was later shown to have significant registry errors at the TMD of the structure (Corringer et al., 2010; Hibbs and Gouaux, 2011; Mnatsakanyan and Jansen, 2013). A new *Torpedo* nAChR cryo-EM structure at 2.7 Å resolution with α-bungarotoxin molecules bound at the orthosteric sites was published during the review process of this work (PDB ID: 6UWZ), which confirmed the previous discrepancies and also pointed to magnification errors with the previous *Torpedo* nAChR structure (Rahman et al., 2020). Therefore, issues with the TMD geometry may also have contributed to the observed discrepancies among the computational studies.

In the following sections, the focus will be on the α7 nAChR structure and properties, and the computational modeling studies on α7 nAChR.

3. Modeling applications to α7 nAChR

3.1. α7 structure and properties

α7 nAChR shares the general features of the heteromeric nAChR but it has mechanistic and structural differences important for its functioning. The homopentameric α7 is distinguished from heteromeric nAChR due to its low probability of opening (Yu and Role, 1998), rapid desensitization (Couturier et al., 1990), high calcium permeability (Séguéla et al., 1993), and five potential orthosteric ligand binding sites on the ECD (Palma et al., 1996).

α7 nAChR has been targeted for the treatment of cognitive symptoms of diseases such as Alzheimer's disease (Wallace et al., 2011), schizophrenia (Beinat et al., 2015; Martin and Freedman, 2007), and depression (Mineur et al., 2017; Zhao et al., 2017). In addition to its function as a traditional ion channel, α7 nAChR is also involved in the cholinergic anti-inflammatory pathway (Borovikova et al., 2000; Wang et al., 2003), and α7 ligands with anti-inflammatory properties have been reported in *in vitro* and *in vivo* studies (Horenstein and Papke, 2017).

Although there is no high-resolution structure for α7 nAChR at the moment, structures of some nAChR homologues and heteromeric nAChR have been solved and serve as templates for construction of homology models. Perhaps the most important nAChR analog for modeling purposes are the acetylcholine binding proteins (AChBP). AChBP is the common name of a group of homopentameric soluble proteins typically found in marine organisms that have ~21–27% sequence similarity to the α7 ECD (Brejc et al., 2001; Celie et al., 2005b; Hansen et al., 2005; Sixma and Smit, 2003; Smit et al., 2001). AChBP are particularly useful for modeling α7 nAChR due to their homopentameric structure, and AChBP structures co-crystallized with various ligands have been used templates for α7 ECD homology models (Fig. 2) (Shahsavar et al., 2015).

In addition to the AChBP, structures of engineered AChBP with 41–71% sequence identity to human α7 ECD (α7-AChBP) have been crystallized with various orthosteric and non-orthosteric ligands (Delbart et al., 2017; Li et al., 2011; Nemecz and Taylor, 2011; Spurny et al., 2015).

3.2. Structural studies with α7 ECD/TMD models

Studies of α7 nAChR prior to 2005 were mostly based on ECD-only models using the HEPES-bound AChBP (Brejc et al., 2001) or *Torpedo* nAChR structure at 9 Å resolution (Unwin, 1995, 1993) as template. The highest-resolution template for the TMD was the *Torpedo* nAChR TMD at 4 Å resolution (Miyazawa et al., 2003). The *Torpedo* nAChR structures at 4 Å resolution (Unwin, 2005; Unwin and Fujiyoshi, 2012) enabled modeling of higher quality homology models including both the ECD and TMD (α7 ECD/TMD).

Two modeling studies focusing on α7 ion channel gating were published within 2005 for chick and human α7 ECD/TMD models. Sampling of the energetics of sodium ion passage from the channel pore through implicit-membrane MD simulations and umbrella sampling calculations with chick α7 ECD/TMD identified the region of the ion pore between T6′, L9′, and V13′ as the narrowest region with E20′ as a free energy well that played a role in ion selectivity of the receptor (Amiri et al., 2005). Explicit-membrane MD simulations with an apo state human α7 ECD/TMD model showed subunit asymmetry caused by the displacement of two non-adjacent subunits. In addition, opening of the C-loop showed a correlated motion with ~10° counterclockwise rotation at the M2 domain of the TMD involving the residues L9′, V13′, and L17' (Law et al., 2005) (Fig. 3, right panel).

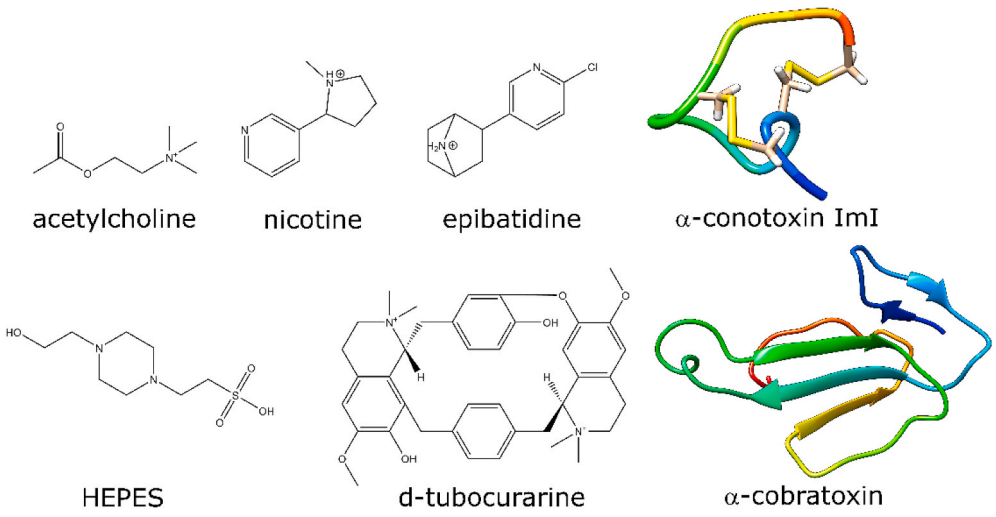

Fig. 2. Molecules commonly used in *in silico* studies or co-crystallized with α7 analogs.

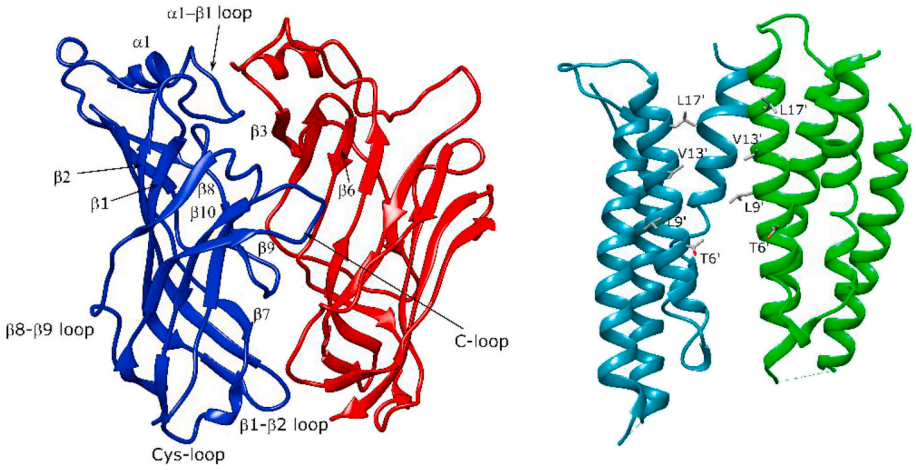

Fig. 3. Structural domains of the α7 ECD (left panel) and important TMD residues (right panel).

The α7 channel opening mechanism was investigated by Cheng et al. in three related studies with an α7 ECD/TMD model through implicit-membrane MD simulations and NMA calculations (Cheng et al., 2006a), explicit-membrane Ta-MD simulations (Cheng et al., 2006b), and explicit-membrane MD and PCA calculations (Cheng et al., 2007). The channel opening mechanism depicted by the results of the three studies was a highly intertwined one. Channel opening was triggered by C-loop closure, which resulted in a global twisting motion involving the β1-β2 loop, β8-β9 loop, and the β10-M1 junction (Fig. 3, left panel). Twisting at these domains reduced the distance between the Cys-loop and the β10-M1 junction (Ta-MD) and/or the Cys- and β1-β2 loops (PCA). Coupling between these loops and the M2-M3 linker of the TMD caused a downward tilt that expanded to the M2 and M3 helices through a clockwise rotation of the M2 helices by ~7°, which in turn resulted in channel opening through removal of the residues L9′ and V13' from the channel pore (Cheng et al., 2006b) similar to the MD simulations of Law et al. (2005).

The putative open (Chiodo et al., 2015), desensitized (Chiodo et al., 2017), and closed state (Chiodo et al., 2018) structures of α7 ECD/TMD revealed significant differences among the three states. The global quaternary twist angle distributions calculated were 20° for the open state, 24° for the desensitized state, and 25° for the closed state. The global twisting motion had an effect on the distances between the Cys-loop and the M2-M3 linker, which was ~2 Å larger in the desensitized and ~2.5 Å larger in the closed state compared to the open state. In addition, the distance between the M2-M3 linker and the β1-β2 loop was 2 Å larger in the closed state compared to the open state.

The arrangement of the M2 helices were parallel in the desensitized model, which tilted into a V-like conformation in the open state model that better allowed passage of water and ions, and an inverted-V-like conformation in the closed state model that mostly blocked the ion channel. The pore radius around the residues L9′, L16′, and E20' gradually decreased through the open (~5 Å), desensitized (~2 Å), and closed states (<2 Å), which was also reflected by the decrease in the number of water molecules. The average number of water molecules in the ion channel were 50% lower in the desensitized state and 90% lower in the closed state compared to the open state. The presence of water molecules in the ion channel and the predicted closed channel pore radius of 2 Å is consistent with the findings of early studies with α7 TMD models (Sankararamakrishnan et al., 1996; Sansom et al., 1995).

Partial channel opening and C-loop closure triggered by high concentrations of Ca^{2+} ions has been proposed based on MD simulations and umbrella sampling calculations with α7 ECD/TMD (Suresh and Hung, 2019). The ECD residues implicated with Ca^{2+} interactions were consistent with the residues identified in past electrophysiology experiments (Galzi et al., 1996). At the TMD, the presence of Ca^{2+} ions were associated with a sharp root mean square deviation (RMSD) increase at the M2-M3 linker and shifting of the M2 helices towards the M3 helices.

The energy barrier for Ca^{2+} passage from the ion channel was ~10 kcal/mol lower in the Ca^{2+}-added simulations compared to the Ca^{2+}-free calculations implying a more accessible ion channel.

3.3. Structural studies with α7 ECD models

Studies with α7 ECD homology models with fivefold occupancy showed stability differences and subunit asymmetry in multiple studies measured by RMSD and root mean square fluctuation (RMSF) differences among the individual subunits of the protein. The symmetrizing and stabilizing effect of agonist binding on the α7 ECD was observed in MD simulations with apo, ACh- (agonist), ACh plus Ca^{2+} (agonist + potentiator), and D-tubocurarine-bound (antagonist) α7 ECD models (Henchman et al., 2005, 2003). The asymmetric motions of the antagonist-bound and apo structures were argued by the authors to be functionally relevant through hindering the ion flow at the α7 ECD vestibule. On the other hand, symmetrizing effect of ACh binding was also reported in MD simulations with AChBP that does not have an ion channel (Gao et al., 2005), so the importance of this symmetrization is not clear.

Interestingly, increased α7 ECD symmetry was observed in antagonist α-cobratoxin-bound simulations as well, although at a lesser extent (Yi et al., 2008). Further, asymmetric clockwise tilting of a single subunit by ~10° during the apo MD simulations resulted in a swing motion that involved C- and F-loop residues. The residues involved in this motion were previously shown to go through large structural movements upon receptor activation in SCAM experiments (Lyford et al., 2003; McLaughlin et al., 2007), which led the authors to the conclusion that spontaneous asymmetric motions in the absence of an agonist may lead to the formation of subunits with "open conformations" similar to the conformation of agonist-bound subunits.

3.4. Ligand binding to α7 orthosteric site

A key question in α7 ECD studies is the role of the C-loop in ligand binding and receptor activation. SMD simulations and potential of mean force (PMF) calculations to determine the mechanism of ACh dissociation from the α7 ECD orthosteric site and the residues involved in dissociation identified the lowest-energy dissociation pathway as ACh sliding under the C-loop in a direction parallel to the membrane (Zhang et al., 2006).[1] Dissociation resulted in loss of interactions with Y93, Y188, W149, and the negative face residue W55, consistent with the mutagenesis and fluorescence-quenching studies with the α7 receptor (Gao et al., 2005; Puskar et al., 2011; Van Arnam et al., 2013; Williams et al., 2009).

α-conotoxins are 12–20 amino acid peptides that act as competitive inhibitors of nAChR (Lebbe et al., 2014; Nasiripourdori et al., 2011). The lowest-energy dissociation pathway of α-conotoxin ImI from the α7 orthosteric site calculated by RAMD and SMD calculations with α7 ECD was parallel to the C-loop similar to the mechanism proposed for ACh Zhang et al. but the residues involved in ligand binding were not the same. Contrary to the case of ACh that formed interactions with the aromatic cage residues of the positive face, α-conotoxin ImI formed hydrogen bonds with the negative face residues D197, E162, and D164, plus π-cation interactions with Y195 (Yu et al., 2012).

The importance of steric factors in α-conotoxin ImI binding was observed in MD simulations with α-conotoxin ImI-bound α7 ECD mutants N111S, Q117S, Q117A, P120A, and G153S (Yu et al., 2011). These mutants were shown to have altered binding affinities to α-conotoxin ImI (Quiram and Sine, 1998), which correlated with disruption or improvement of packing at the interface between α-conotoxin ImI and α7 ECD during the MD simulations for all mutants except N111S, which could not be accounted for.

The correlation between ligand mode of action and C-loop opening distances was explored with MD simulations and umbrella sampling calculations using α7 ECD models bound to agonists, antagonists, and partial agonists (Tabassum et al., 2017). The lowest agonist binding energies were observed when the C-loop was mostly closed and lower antagonist energies were observed when the C-loop was mostly open, although the energy barriers of 1–2 kcal/mol could not be considered significant in MD simulations. As a result, the authors suggested ligand dissociation profiles as a metric to predict mode of action of α7 ligands rather than the binding energies.

The predicted binding configuration of α7 agonists in docking calculations with the α7 ECD was proposed as a way to predict ligand selectivity, potency and activity (Xiao et al., 2012). Ligands interacting with the residues Y195, W149, Y93, and L119 such as epibatidine, nicotine, and varenicline were proposed to be non-selective and high-affinity α7 agonists. Ligands with additional interactions with the negative face Q117 were proposed to be moderate α7 affinity and selectivity, and interactions with the D- and F-loop residues were attributed to ligands with high α7 affinity and specificity.

Another important aspect of α7 binding studies is prediction of ligand binding energies. Molecular Mechanics Poisson-Boltzmann Surface Area (MMPBSA) and Molecular Mechanics Generalized Born Surface Area (MMGBSA) are two methods commonly used to calculate ligand binding energies. They use continuum electrostatics to calculate the polar solvation energy and an empirical function to calculate the nonpolar solvation energy (Genheden and Ryde, 2015). Docking of eight α7 agonists (Grazioso et al., 2008, Table 1) to an α7 ECD model followed by MD simulations and MMPBSA calculations with different atomic parameters and energy calculation software yielded binding energies within 1–2 kcal/mol of the experimental binding energies for the best-performing method with an $R^2 = 0.69$ (Grazioso et al., 2008).

In another study, a modified MMPBSA method (Ferrari et al., 2007) using an α7 ECD model relaxed through structure minimization rather than MD simulations for the binding energy calculations showed good correlation between the calculated and experimental energies for a set of sixteen known α7 agonists in a training set ($R^2 = 0.81$), but the binding energies calculated for six novel α7 agonists (Grazioso et al., 2009, Fig. 3) that were designed based on the lowest-energy fragments in the training set showed no correlation with the experimental energies (Grazioso et al., 2009).

MMPBSA and MMGBSA calculations were used in another study on α-conotoxin ImI-bound α7 ECD following MD simulations to predict the effect of α-conotoxin ImI mutations on α7 binding. When tested on sixteen α-conotoxin ImI mutants, the best correlation ($R^2 = 0.69$) with the experimental binding energies was found for the MMGBSA calculations (Yu et al., 2011).

3.5. α7 allosteric ligand binding

The activity of α7 nAChR can be modulated by a large number of ligands. α7 positive allosteric modulators (PAMs) are ligands that have no activity when applied by themselves but potentiate agonist responses upon co-application (Supporting Fig. 1). Two classes of α7 PAMs were defined based on their effect on the desensitized states of the receptor (Grønlien et al., 2007; Williams et al., 2011). Type I PAMs like NS-1738 (Timmermann et al., 2007) and 5-HI (Zwart et al., 2002) increase current peak amplitudes with no apparent effect on receptor desensitization, whereas type II PAMs like TQS (Grønlien et al., 2007) and PNU-120596 (Hurst et al., 2005) can recover the receptor from the non-conductive D_s state. The proposed binding site for PAMs is in the TMD based on mutagenesis and docking studies (Collins et al., 2011; Young et al., 2008).

Different than the type I and II PAMs, agonist-positive allosteric modulators (ago-PAMs) such as GAT107 (Gill et al., 2011; Thakur et al.,

[1] Note that in a reversible process, one can model it from either direction. Dissociation is usually preferred because it is computationally less intensive than modeling association.

Table 1
List of the simulation times, membrane models, template references and template names for the studies reviewed in this study. NA indicates the particular parameter does not apply to that model. The templates of the α7 ECD/TMD models were split such that the structure on the left hand side is the template for the ECD and the right hand side is the template for the TMD. *Ac* symbol in the template names stands for *Aplysia californica* and *Ls* stands for *Lymnaea stagnalis*.

Reference	Time (ns)	Membrane Model	Template Reference	Template name
Amiri et al. (2005)	60	Implicit	(Brejc et al., 2001)/(Miyazawa et al., 2003)	HEPES-bound *Ls*-AChBP/*Torpedo* nAChR TMD
Bisson et al. (2008)	0.5	NA	Brejc et al. (2001)	HEPES-bound *Ls*-AChBP
Cheng et al. (2006a)	1	Implicit	(Brejc et al., 2001)/(Miyazawa et al., 2003)	HEPES-bound *Ls*-AChBP/*Torpedo* nAChR TMD
Cheng et al. (2006b)	2	POPC	(Hansen et al., 2005)/(Unwin, 2005)	Epibatidine-bound *Ac*-AChBP/*Torpedo* nAChR
Cheng et al. (2007)	2	POPC	Unwin (2005)	*Torpedo* nAChR
Chiodo et al. (2015)	200	POPC	(Hansen et al., 2005)/(Hibbs and Gouaux, 2011)	Epibatidine-bound *Ac*-AChBP/*C. elegans* GluCl
Chiodo et al. (2017)	200	POPC	(Hansen et al., 2005)/(Hibbs and Gouaux, 2011)	Epibatidine-bound *Ac*-AChBP/*C. elegans* GluCl
Chiodo et al. (2018)	200	POPC	(Hansen et al., 2005)/(Hibbs and Gouaux, 2011)	α-conotoxin ImI-bound/*C.elegans* GluCl
Grazioso et al. (2008)	5	NA	Hansen et al. (2005)	Epibatidine-bound *Ac*-AChBP
Grazioso et al. (2009)	NA	NA	Hansen et al. (2005)	Epibatidine-bound *Ac*-AChBP
Grazioso et al. (2015)	500	POPC	(Hansen et al., 2005)/(Unwin, 2005)	Epibatidine-bound *Ac*-AChBP/*Torpedo* nAChR
Gulsevin et al. (2019)	20	NA	Li et al. (2011)	Epibatidine-bound α7-AChBP
Henchman et al. (2003)	10	NA	Brejc et al. (2001)	HEPES-bound *Ls*-AChBP
Henchman et al. (2005)	15	NA	Brejc et al. (2001)	HEPES-bound *Ls*-AChBP
Horenstein et al. (2016)	50	NA	Li et al. (2011)	Epibatidine-bound α7-AChBP
Huang et al. (2006)	13	NA	Celie et al. (2004)	Nicotine-bound *Ls*-AChBP
Huang et al. (2008)	6.5	NA	Celie et al. (2004)	Nicotine-bound *Ls*-AChBP
Kombo and Bencherif (2013)	NA	NA	Hansen et al. (2005)	Epibatidine-bound *Ac*-AChBP
Law et al. (2005)	15	POPC	(Brejc et al., 2001)/(Miyazawa et al., 2003)	HEPES-bound *Ls*-AChBP/*Torpedo* nAChR TMD
Leffler et al. (2017)	NA	NA	(Celie et al., 2005a; Dutertre et al., 2007; Hansen et al., 2005; Ulens et al., 2006)	α-conotoxin-bound AChBP
Newcombe et al. (2018)	NA	NA	(Unwin, 2005; Unwin and Fujiyoshi, 2012)	Refined *Torpedo* nAChR
Quadri et al. (2019)	200	POPC	(Li et al., 2011)/(Morales-Perez et al., 2016)	Epibatidine-bound α7-AChBP/α4β2 nAChR
Sankararamakrishnan et al. (1996)	0.5	Implicit	Unwin (1995)	9 Å *Torpedo* nAChR
Sansom et al. (1995)	0.5	Implicit	(Unwin, 1995, 1993)	9 Å *Torpedo* nAChR
Suresh and Hung (2016)	45–65	NA	Celie et al. (2005a)	α-conotoxin PnIA variant-bound *Ac*-AChBP
Suresh and Hung (2019)	45–65	DOPC	Unwin (2005)	*Torpedo* nAChR
Tabassum et al. (2017)	60	NA	Ulens et al. (2006)	α-conotoxin ImI-bound *Ac*-AChBP
Targowska-Duda et al. (2018)	100	POPC	Hassaine et al. (2014)	5-HT_{3A}R
Xiao et al. (2012)	NA	NA	Hansen et al. (2005)	Epibatidine-bound *Ac*-AChBP
Yi et al. (2008)	32.6	NA	Bourne et al. (2005)	α-cobratoxin bound *Ls*-AChBP
Yu et al. (2011)	10.5	NA	(Dellisanti et al., 2007; Ulens et al., 2006)/(Unwin, 2005)	α1 ECD and α-conotoxin ImI bound *Ac*-AChBP/*Torpedo* nAChR
Yu et al. (2012)	7	NA	(Dellisanti et al., 2007; Ulens et al., 2006)/(Unwin, 2005)	α1 ECD and α-conotoxin ImI bound *Ac*-AChBP/*Torpedo* nAChR
Zhang et al. (2006)	1	NA	Brejc et al. (2001)	HEPES-bound *Ls*-AChBP

2013) and B–973B (Garai et al., 2018; Post-Munson et al., 2017) activate α7 when applied by themselves through direct allosteric activation (DAA) and act as type II PAMs when co-applied with orthosteric agonists (Supporting Fig. 1). GAT107 was originally proposed to exert DAA through the TMD PAM site based on docking and mutation studies (Collins et al., 2011; Gill et al., 2011; Young et al., 2008). The mechanism of activation was explained by C-loop closure upon GAT107 binding at the TMD PAM site based on explicit-membrane MD simulations and metadynamics calculations with an α7 ECD/TMD model (Grazioso et al., 2015). However, the plausibility of this mechanism is challenged by the observations that GAT107 can activate α7 mutants with no functional orthosteric sites and the DAA activity can be selectively blocked by antagonists such as 2,3,5,6 MP-TQS (Gill-Thind et al., 2015) without affecting its PAM activity (Horenstein et al., 2016; Papke et al., 2014).

To explain these observations, a second binding site on the ECD was explored through docking calculations covering the vestibular space behind the orthosteric site (Horenstein et al., 2016) based on ligand binding at this vestibular site in α7-AChBP crystal structures (Spurny et al., 2015). GAT107 docked to the region surrounded by the residues L56, M58, K87, I90, L92, F100, A102, Y118, P120 with the residues R99 and D101 of the neighboring vestibules forming salt bridge at the rim of the binding site. Inhibition of GAT107 DAA by disruption of this salt bridge through the D101A mutation and blocking of this site with MTSEA treatment of the α7D101C mutant lend support to ago-PAM binding at the vestibular site. Later docking calculations with B–973B also showed poses at the identified DAA site (Quadri et al., 2019).

Although most computational studies involving PAMs utilize the TMD PAM site defined in earlier studies (Collins et al., 2011; Young et al., 2008), the structure and location of this site was revisited in multiple studies following the reports of an error in assignment of the M1 helix of the *Torpedo* nAChR structure used to propose the TMD PAM binding site (Corringer et al., 2010; Hibbs and Gouaux, 2011; Mnatsakanyan and Jansen, 2013).

Consensus docking calculations with the analogs of type II PAMs A-867744 (Faghih et al., 2009; Malysz et al., 2009), TBS-516 (Chatzidaki and Millar, 2015), and TQS (Gill-Thind et al., 2015; Gill et al., 2012; Grønlien et al., 2007) (Supporting Fig. 1) to a refined α7 ECD/TMD model identified an intrasubunit site (Newcombe et al., 2018, Fig. 9) defined by the residues L248, S249, and F253 of the negative face subunit, and L247, L248, T251, and M254 positive face subunit, but TBS-516 formed additional interactions with M278 and V281, and A-867744 formed interactions with S222 (Newcombe et al., 2018). Differently, docking of B–973B and GAT107 to the TMD of α7 ECD/TMD showed poses under the M2-M3 linker defined by the residues F253, M254, V257, P269, I271, F275, L215, and C219 of the positive-face subunit and the residues L209, Y210, L213, and N214 of the negative face subunit at a position different than the proposed PAM site, which was consistent with the greater sensitivity of B–973B to the M254L mutation compared to GAT107 because the extended configuration of B–973B would cause clashes with the bulkier leucine residue whereas GAT107 could fit in the pocket in different configurations (Quadri et al., 2019). In a study using the 5-HT_{3A} structure (Hassaine et al., 2014) as the template, docking of type I and type II PAMs to α7 ECD/TMD showed

poses at three different sites whereby the binding site under the M2-M3 linker showed poses for both types of PAMs, the intrasubunit site showed poses of type II PAMs, and the intersubunit site showed poses of type I PAMs (Targowska-Duda et al., 2018). The locations of these sites were consistent with the PAM sites bearing the intrasubunit (Newcombe et al., 2018) and intersubunit sites (Collins et al., 2011; Young et al., 2008) alluded in the previous studies (Targowska-Duda et al., 2018, Figs. 3 and 4).

Most recently, allosteric agonists of α7 that selectively bind at the ECD allosteric site with no TMD site binding were identified in a study where sixteen diethylphenylpiperazine (diEPP) derivative α7 nAChR partial or silent agonists (Quadri et al., 2016) were screened by docking, MD simulations, and MMPBSA calculations (Gulsevin et al., 2019). The two molecules identified as hits (2NDEP and *p*-CF_3 diEPP, Supporting Fig. 1) activated the orthosterically-compromised α7C190A mutant when co-applied with PNU-120596, which was blocked by application of 2,3,5,6 MP-TQS in support of ECD-only binding.

3.6. α7 nAChR comparisons with other nAChR

Because the structure of the α4β2 receptor was solved relatively recently, the majority of the studies comparing α7 and heteromeric nAChR were based on homology modeling using the AChBP or the *Torpedo* nAChR structures as the template. Comparison of α7 and α4β2 ECD homology models to identify the structural differences at the orthosteric sites showed that the α7 orthosteric site is more lipophilic and less negatively charged than that of α4β2, especially around the critical residue W149 (Bisson et al., 2008). Another difference between α7 and α4β2 was identified as long-range electrostatic interactions between the receptor and the ligands through MD simulations and docking calculations. The selectivity of α4β2 agonists to this subtype despite similar docking poses at the orthosteric sites of α7 and α4β2 ECD models was explained by the authors with the greater negative charge of α4β2 ECD ($-37e^-$) compared to the α7 ECD ($-20e^-$) (Huang et al., 2006). A binding energy formula derived by fitting docking energies of ligands that includes long-range electrostatic interactions qualitatively predicted the potency changes of AR-R17779 and 4-OH-GTS-21 associated with the Q117F mutation (Huang et al., 2008).

Screening of α-conotoxin [γ4E]GID single-point mutations at sixteen positions using the FoldX server (Schymkowitz et al., 2005) to find conotoxin variants with increased α4β2 selectivity while maintaining feasible binding energies identified E4R, R12F, and V13R as candidates for experimental studies, but these mutants were not tested experimentally (Suresh and Hung, 2016). Another approach to screen for α-conotoxin GID mutants with increased α4β2 selectivity used the ToxDock protocol that is based on ensemble docking calculations with extensive conformational sampling of the peptide conformations to dock α-conotoxin GID mutants to α4β2 ECD (Leffler et al., 2017). Three α-conotoxin GID mutations (A10V, V13I, and V13Y) were predicted to be bioactive by the algorithm, and two of these peptides (V13I and V13Y) showed decreased α7 and α3β2 nAChR selectivity.

The dissociation pathway of the α-conotoxin GID mutant [γ4E] from α7 and α4β2 ECD investigated through MD simulations and umbrella sampling showed that the initial steps of dissociation from α7 involved interactions mostly with the negative face residues Q27, Q57, and Q161 through a pathway parallel to the C-loop consistent with the studies with α-conotoxin ImI (Yu et al., 2012), whereas dissociation from α4β2 was through a pathway nearly perpendicular to the C-loop with very few interactions with the negative face residues (Suresh and Hung, 2016). The dissociation energy plateau calculated for α7 was 12 kcal/mol higher, which was considered by the authors to be consistent with the higher α7 potency of α-conotoxin GID observed in binding assays (Nicke et al., 2003).

As the final example to ligand binding studies, a Bayesian model trained with binding affinities and six molecular descriptors of small nAChR ligands to predict ligand binding affinities to human and rat α4β2, α7, α3β4, α6β2β3 showed accuracies between 0.65 and 0.83 for the test sets, and human α7 was among the highest-accuracy proteins at 100 nM and 500 nM affinity cutoff (Kombo and Bencherif, 2013). The α7 accuracies from docking calculations were ~0.71, which improved to ~0.82 when a constraint between the charged nitrogen and W149 backbone oxygen was applied.

4. Summary and future directions

In summary, computational structural studies of *Torpedo* nAChR and α7 nAChR yielded valuable information regarding the activation mechanism of nAChR, and the results from ECD-only or TMD-only models were mostly consistent with the results from ECD/TMD models. However, few questions on nAChR mode of action remain open.

C-loop closure has been directly linked to channel opening in some MD studies (Grazioso et al., 2015; Suresh and Hung, 2019; Tabassum et al., 2017), but nAChR mutants with compromised C-loops can still be activated (Gulsevin et al., 2019; Horenstein et al., 2016; Papke et al., 2014; Purohit and Auerbach, 2013). Based on these results, C-loop closure may be one of the involved factors for channel activation, but not the only one. As for symmetry, involvement in receptor activation was suggested based on ECD-only models (Henchman et al., 2005, 2003), but systematic studies exploring the roots and functional role of symmetry in homomeric nAChR activation are necessary to understand its precise role.

Classical MD- and docking-based calculations yielded results that explain the properties of ligands that are chemically related at a qualitative level, but either approach fell short of generating predictive models that apply to a wider range of molecules or the results predicted by the computational models were not tested experimentally. This was the case both for small-molecule ligands (Grazioso et al., 2009, 2008; Huang et al., 2008, 2006; Zhang et al., 2006) and α-conotoxin peptides (Suresh and Hung, 2016; Yu et al., 2012, 2011). On the other hand, computational methods such as statistics-based affinity screening for small molecule ligands (Kombo and Bencherif, 2013) and the ToxDock docking protocol to overcome conformational sampling issues associated with peptide ligands (Leffler et al., 2017) performed better in predicting the relative binding energies of α7 ligands, which should be utilized more frequently.

Computational studies on α7 nAChR also led to the identification of novel allosteric sites on the receptor and the mode of action of these ligands. Multiple proposals have been made regarding the position of TMD PAM binding site (Collins et al., 2011; Newcombe et al., 2018; Quadri et al., 2019; Targowska-Duda et al., 2018; Young et al., 2008), but the compact structure of the α7 TMD makes experimental validation of these predictions problematic. The ECD allosteric site (or better a site equivalent to it) has been previously observed in α7-AChBP crystal structures (Delbart et al., 2017; Spurny et al., 2015), docking studies with α7-AChBP (Kuang et al., 2016) and α4β2 ECD (Arias et al., 2015), but only recently has been confirmed as the binding site of ago-PAMs GAT107, B–973B, and allosteric agonist diEPP derivatives (Gulsevin et al., 2019; Horenstein et al., 2016; Quadri et al., 2019).

In the light of these results, a few factors stand out for the ongoing success of the computational studies. The first one is the simulation timescales. The advancements in the GPU technology drastically increased timescales affordable in MD simulations. The putative open, closed, and desensitized states of the receptor were obtained through MD simulations at the timescale of hundreds of nanoseconds. Considering the changes observed in these calculations compared to the shorter MD simulations, longer MD simulations should be run to better sample the nAChR dynamics. Recent results from MD simulations with the α4β2 crystal structure showed that independent simulations can result in significantly different trajectories (Yu et al., 2019) suggesting that the results averaged from replicate simulations or application of statistical methods are likely to be more reliable compared to the results of a single simulation.

Secondly, binding energy calculations of ligands posed at a single, arbitrary interface of homomeric nAChR does not yield reliable results and thus should be abandoned in favor of considering all protein subunits in the analyses. Because orthosteric sites can go through stochastic changes throughout the MD simulations, comparison of ligand poses at structurally similar orthosteric sites can improve the correlation between the calculated and measured energies (Gulsevin, 2017).

Thirdly, availability of new structures enables better analysis of certain nAChR subtypes and also allow building of better homology models. Examples to these new structures include α4β2 nAChR (Morales-Perez et al., 2016; Walsh et al., 2018), α3β4 nAChR (Gharpure et al., 2019), and more recently, the muscle-type *Torpedo* nAChR (Rahman et al., 2020). The α4β2 receptor has higher homology to α7 nAChR in comparison to the Torpedo nAChR, and thus may be a more reliable template for the modeling of the α7 TMD. The α3β4 and new *Torpedo* nAChR structures include a portion of the ICD, which can be used to build improved nAChR models involving the ICD. Finally, the new *Torpedo* nAChR structure gives a more accurate view of the protein, particularly at the TMD and the F-loop that was missing in the previous *Torpedo* nAChR structure, which will allow more accurate computational analyses on this protein.

Overall, studies on nAChR revealed many important aspects of nAChR activation and provided information on ligand modes of action. The aim of this review was to lay out the results from computational studies to give a concise summary of the predicted mechanisms of nAChR activation, prediction of ligand – nAChR interactions, and allosteric activation mechanisms. The validity and the success of these methods were analyzed based on experimental and other computational studies. It is hoped that the conclusions from the results of these studies will be useful in future modeling studies with the nicotinic acetylcholine receptors.

CRediT authorship contribution statement

Alican Gulsevin: Conceptualization, Data curation, Formal analysis, Investigation, Methodology, Project administration, Resources, Supervision, Validation, Visualization, Writing - original draft, Writing - review & editing.

Acknowledgements

This work was supported by the National Institutes of Health (NIH) through grants R01 GM080403 and R01 HL144131. The author would like to thank Dr. Nicole A. Horenstein for her valuable comments on the manuscript.

Appendix A. Supplementary data

Supplementary data to this article can be found online at https://doi.org/10.1016/j.neuropharm.2020.108257.

References

Adcock, S.A., McCammon, J.A., 2006. Molecular dynamics: survey of methods for simulating the activity of proteins. Chem. Rev. 106, 1589–1615. https://doi.org/10.1021/cr040426m.

Amiri, S., Tai, K., Beckstein, O., Biggin, P.C., Sansom, M.S.P., 2005. The α7 nicotinic acetylcholine receptor: molecular modelling, electrostatics, and energetics. Mol. Membr. Biol. 22, 151–162. https://doi.org/10.1080/09687860500063340.

Arias, H.R., Feuerbach, D., Targowska-Duda, K., Kaczor, A.A., Poso, A., Jozwiak, K., 2015. Pharmacological and molecular studies on the interaction of varenicline with different nicotinic acetylcholine receptor subtypes. Potential mechanism underlying partial agonism at human α4β2 and α3β4 subtypes. Biochim. Biophys. Acta Biomembr. 1848, 731–741. https://doi.org/10.1016/j.bbamem.2014.11.003.

Baenziger, J.E., Hénault, C.M., Therien, J.P.D., Sun, J., 2015. Nicotinic acetylcholine receptor-lipid interactions: mechanistic insight and biological function. Biochim. Biophys. Acta Biomembr. 1848, 1806–1817. https://doi.org/10.1016/j.bbamem.2015.03.010.

Bahar, I., Lezon, T.R., Bakan, A., Shrivastava, I.H., 2010. Normal mode analysis of biomolecular structures: functional mechanisms of membrane proteins. Chem. Rev. 110, 1463–1497. https://doi.org/10.1021/cr900095e.

Beinat, C., Banister, S.D., Herrera, M., Law, V., Kassiou, M., 2015. The therapeutic potential of α7 nicotinic acetylcholine receptor (α7 nAChR) agonists for the treatment of the cognitive deficits associated with schizophrenia. CNS Drugs 29, 529–542. https://doi.org/10.1007/s40263-015-0260-0.

Belfield, W.J., Cole, D.J., Martin, I.L., Payne, M.C., Chau, P.L., 2014. Constrained geometric simulation of the nicotinic acetylcholine receptor. J. Mol. Graph. Model. 52, 1–10. https://doi.org/10.1016/j.jmgm.2014.05.001.

Bertrand, D., Bertrand, S., Cassar, S., Gubbins, E., Li, J., Gopalakrishnan, M., 2008. Positive allosteric modulation of the α7 nicotinic acetylcholine receptor: ligand interactions with distinct binding sites and evidence for a prominent role of the M2-M3 segment. Mol. Pharmacol. 74, 1407–1416. https://doi.org/10.1124/mol.107.042820.nitive/attention.

Bisson, W.H., Westera, G., Schubiger, P.A., Scapozza, L., 2008. Homology modeling and dynamics of the extracellular domain of rat and human neuronal nicotinic acetylcholine receptor subtypes α4β2 and α7. J. Mol. Model. 14, 891–899. https://doi.org/10.1007/s00894-008-0340-x.

Blount, P., Merlie, J.P., 1989. Molecular basis of the two nonequivalent ligand binding sites of the muscle nicotinic acetylcholine receptor. Neuron 3, 349–357. https://doi.org/10.1016/0896-6273(89)90259-6.

Borovikova, L.V., Ivanova, S., Zhang, M., Yang, H., Botchkina, G.I., Watkins, L.R., Wang, H., Abumrad, N., Eaton, J.W., Tracey, K.J., 2000. Vagus nerve stimulation attenuates the systemic inflammatory response to endotoxin. Nature 405, 458–462. https://doi.org/10.1038/35013070.

Bourne, Y., Talley, T.T., Hansen, S.B., Taylor, P., Marchot, P., 2005. Crystal structure of a Cbtx-AChBP complex reveals essential interactions between snake α-neurotoxins and nicotinic receptors. EMBO J. 24, 1512–1522. https://doi.org/10.1038/sj.emboj.7600620.

Bouzat, C., Gumilar, F., Spitzmaul, G., Wang, H.-L., Rayes, D., Hansen, S.B., Taylor, P., Sine, S.M., 2004. Coupling of agonist binding to channel gating in an ACh-binding protein linked to an ion channel. Nature 430, 896–900.

Brejc, K., Van Dijk, W.J., Klaassen, R.V., Schuurmans, M., Van Der Oost, J., Smit, A.B., Sixma, T.K., 2001. Crystal structure of an ACh-binding protein reveals the ligand-binding domain of nicotinic receptors. Nature 411, 269–276. https://doi.org/10.1038/35077011.

Brooks, B., Karplus, M., 1985. Normal modes for specific motions of macromolecules: application to the hinge-bending mode of lysozyme. Proc. Natl. Acad. Sci. U.S.A. 82, 4995–4999. https://doi.org/10.1073/pnas.82.15.4995.

Cecchini, M., Changeux, J.-P., 2014. The nicotinic acetylcholine receptor and its prokaryotic homologues: structure, conformational transitions & allosteric modulation. Neuropharmacology 96, 1–13. https://doi.org/10.1016/j.neuropharm.2014.12.006.

Celie, P.H.N., Kasheverov, I.E., Mordvintsev, D.Y., Hogg, R.C., van Nierop, P., van Elk, R., van Rossum-Fikkert, S.E., Zhmak, M.N., Bertrand, D., Tsetlin, V., Sixma, T.K., Smit, A.B., 2005a. Crystal structure of nicotinic acetylcholine receptor homolog AChBP in complex with an alpha-conotoxin PnIA variant. Nat. Struct. Mol. Biol. 12, 582–588. https://doi.org/10.1038/nsmb951.

Celie, P.H.N., Klaassen, R.V., Van Rossum-Fikkert, S.E., Van Elk, R., Van Nierop, P., Smit, A.B., Sixma, T.K., 2005b. Crystal structure of acetylcholine-binding protein from *Bulinus truncatus* reveals the conserved structural scaffold and sites of variation in nicotinic acetylcholine receptors. J. Biol. Chem. 280, 26457–26466. https://doi.org/10.1074/jbc.M414476200.

Celie, P.H.N., Van Rossum-Fikkert, S.E., Van Dijk, W.J., Brejc, K., Smit, A.B., Sixma, T.K., 2004. Nicotine and carbamylcholine binding to nicotinic acetylcholine receptors as studied in AChBP crystal structures. Neuron 41, 907–914. https://doi.org/10.1016/S0896-6273(04)00115-1.

Changeux, J.P., 2012. The nicotinic acetylcholine receptor: the founding father of the pentameric ligand-gated ion channel superfamily. J. Biol. Chem. 287, 40207–40215. https://doi.org/10.1074/jbc.R112.407668.

Chatzidaki, A., Millar, N.S., 2015. Allosteric modulation of nicotinic acetylcholine receptors. Biochem. Pharmacol. https://doi.org/10.1016/j.bcp.2015.07.028.

Cheng, X., Ivanov, I., Wang, H., Sine, S.M., McCammon, J.A., 2007. Nanosecond-timescale conformational dynamics of the human α7 nicotinic acetylcholine receptor. Biophys. J. 93, 2622–2634. https://doi.org/10.1529/biophysj.107.109843.

Cheng, X., Lu, B., Grant, B., Law, R.J., McCammon, J.A., 2006a. Channel opening motion of α7 nicotinic acetylcholine receptor as suggested by normal mode analysis. J. Mol. Biol. 355, 310–324. https://doi.org/10.1016/j.jmb.2005.10.039.

Cheng, X., Wang, H., Grant, B., Sine, S.M., McCammon, J.A., 2006b. Targeted molecular dynamics study of C-loop closure and channel gating in nicotinic receptors. PLoS Comput. Biol. 2, 1173–1184. https://doi.org/10.1371/journal.pcbi.0020134.

Chiara, D.C., Hamouda, A.K., Ziebell, M.R., Mejia, L.A., Garcia, G., Cohen, J.B., 2009. [3H]chlorpromazine photolabeling of the Torpedo nicotinic acetylcholine receptor identifies two state-dependent binding sites in the ion channel. Biochemistry 48, 10066–10077. https://doi.org/10.1021/bi901271w.

Chiodo, L., Malliavin, T.E., Giuffrida, S., Maragliano, L., Cottone, G., 2018. Closed-locked and apo-resting state structures of the human α7 nicotinic receptor: a computational study. J. Chem. Inf. Model. 58, 2278–2293.

Chiodo, L., Malliavin, T.E., Maragliano, L., Cottone, G., 2017. A possible desensitized state conformation of the human α7 nicotinic receptor: a molecular dynamics study. Biophys. Chem. 229, 99–109. https://doi.org/10.1016/j.bpc.2017.06.010.

Chiodo, L., Malliavin, T.E., Maragliano, L., Cottone, G., Ciccotti, G., 2015. A structural model of the human α7 nicotinic receptor in an open conformation. PloS One 10, 1–30. https://doi.org/10.1371/journal.pone.0133011.

Cohen, B.N., Labarca, C., Davidson, N., Lester, H.A., 1992. Mutations in M2 alter the selectivity of the mouse nicotinic acetylcholine receptor for organic and alkali metal cations. J. Gen. Physiol. 100, 373–400. https://doi.org/10.1085/jgp.100.3.373.

Collins, T., Young, G.T., Millar, N.S., 2011. Competitive binding at a nicotinic receptor transmembrane site of two α7-selective positive allosteric modulators with differing effects on agonist-evoked desensitization. Neuropharmacology 61, 1306–1313. https://doi.org/10.1016/j.neuropharm.2011.07.035.

Corringer, P.J., Baaden, M., Bocquet, N., Delarue, M., Dufresne, V., Nury, H., Prevost, M., Van Renterghem, C., 2010. Atomic structure and dynamics of pentameric ligand-gated ion channels: new insight from bacterial homologues. J. Physiol. 588, 565–572. https://doi.org/10.1113/jphysiol.2009.183160.

Couturier, S., Bertrand, D., Matter, J.M., Hernandez, M.C., Bertrand, S., Millar, N., Valera, S., Barkas, T., Ballivet, M., 1990. A neuronal nicotinic acetylcholine receptor subunit (α7) is developmentally regulated and forms a homo-oligomeric channel blocked by α-BTX. Neuron 5, 847–856. https://doi.org/10.1016/0896-6273(90)90344-F.

Delbart, F., Brams, M., Gruss, F., Noppen, S., Peigneur, S., Boland, S., Chaltin, P., Brandao-Neto, J., von Delft, F., Touw, W.G., Joosten, R., Liekens, S., Tytgat, J., Ulens, C., 2017. An allosteric binding site of the α7 nicotinic acetylcholine receptor revealed in a humanized acetylcholine binding protein. J. Biol. Chem. 293 https://doi.org/10.1074/jbc.M117.815316.

Dellisanti, C.D., Yao, Y., Stroud, J.C., Wang, Z.-Z., Chen, L., 2007. Crystal structure of the extracellular domain of nAChR α1 bound to α-bungarotoxin at 1.94 Å resolution. Nat. Neurosci. 10, 953–962. https://doi.org/10.1038/nn1942.

Dutertre, S., Ulens, C., Büttner, R., Fish, A., van Elk, R., Kendel, Y., Hopping, G., Alewood, P.F., Schroeder, C., Nicke, A., Smit, A.B., Sixma, T.K., Lewis, R.J., 2007. AChBP-targeted α-conotoxin correlates distinct binding orientations with nAChR subtype selectivity. EMBO J. 26, 3858–3867. https://doi.org/10.1038/sj.emboj.7601785.

Elgoyhen, A.B., Johnson, D.S., Boulter, J., Vetter, D.E., Heinemann, S., 1994. α9: an acetylcholine receptor with novel pharmacological properties expressed in rat cochlear hair cells. Cell 79, 705–715. https://doi.org/10.1016/0092-8674(94)90555-X.

Faghih, R., Gopalakrishnan, S.M., Gronlien, J.H., Malysz, J., Briggs, C.A., Wetterstrand, C., Ween, H., Curtis, M.P., Sarris, K.A., Gfesser, G.A., El-Kouhen, R., Robb, H.M., Radek, R.J., Marsh, K.C., Bunnelle, W.H., Gopalakrishnan, M., 2009. Discovery of 4-(5-(4-Chlorophenyl)-2-methyl-3-propionyl-1H-pyrrol-1-yl) benzenesulfonamide (A-867744) as a novel positive allosteric modulator of the α7 nicotinic acetylcholine receptor. J. Med. Chem. 52, 3377–3384. https://doi.org/10.1021/jm9003818.

Ferrari, A.M., Degliesposti, G., Sgobba, M., Rastelli, G., 2007. Validation of an automated procedure for the prediction of relative free energies of binding on a set of aldose reductase inhibitors. Bioorg. Med. Chem. 15, 7865–7877. https://doi.org/10.1016/j.bmc.2007.08.019.

Filatov, G.N., White, M.M., 1995. The role of conserved leucines in the M2 domain of the acetylcholine receptor in channel gating. Mol. Pharmacol. 48, 379–384.

Furois-Corbin, S., Pullman, A., 1991. The effect of point mutations on energy profiles in a model of the nicotinic acetylcholine receptor (AChR) channel. Biophys. Chem. 39, 153–159. https://doi.org/10.1016/0301-4622(91)85017-K.

Galzi, J.L., Bertrand, S., Corringer, P.J., Changeux, J.P., Bertrand, D., 1996. Identification of calcium binding sites that regulate potentiation of a neuronal nicotinic acetylcholine receptor. EMBO J. 15, 5824–5832. https://doi.org/10.1002/j.1460-2075.1996.tb00969.x.

Gao, F., Bren, N., Burghardt, T.P., Hansen, S., Henchman, R.H., Taylor, P., McCammon, J.A., Sine, S.M., 2005. Agonist-mediated conformational changes in acetylcholine-binding protein revealed by simulation and intrinsic tryptophan fluorescence. J. Biol. Chem. 280, 8443–8451. https://doi.org/10.1074/jbc.M412389200.

Garai, S., Raja, K.S., Papke, R.L., Deschamps, J.R., Damaj, M.I., Thakur, G.A., 2018. B-973, a novel α7 nAChR Ago-PAM: racemic and asymmetric synthesis, electrophysiological studies, and in vivo evaluation. ACS Med. Chem. Lett. 9, 1144–1148. https://doi.org/10.1021/acsmedchemlett.8b00407.

Genheden, S., Ryde, U., 2015. The MM/PBSA and MM/GBSA methods to estimate ligand-binding affinities. Expet Opin. Drug Discov. 10, 449–461. https://doi.org/10.1517/17460441.2015.1032936.

Gharpure, A., Teng, J., Zhuang, Y., Noviello, C.M., Walsh, R.M., Cabuco, R., Howard, R. J., Zaveri, N.T., Lindahl, E., Hibbs, R.E., 2019. Agonist selectivity and ion permeation in the α3β4 ganglionic nicotinic receptor. Neuron 104, 501–511. https://doi.org/10.1016/j.neuron.2019.07.030 e6.

Gill-Thind, J.K.K., Dhankher, P., D'Oyley, J.M., Sheppard, T.D., Millar, N.S., 2015. Structurally similar allosteric modulators of α7 nicotinic acetylcholine receptors exhibit five distinct pharmacological effects. J. Biol. Chem. 290, 3552–3562. https://doi.org/10.1074/jbc.M114.619221.

Gill, J.K., Dhankher, P., Sheppard, T.D., Sher, E., Millar, N.S., 2012. A series of α7 nicotinic acetylcholine receptor allosteric modulators with close chemical similarity but diverse pharmacological properties. Mol. Pharmacol. 81, 710–718. https://doi.org/10.1124/mol.111.076026.

Gill, J.K., Savolainen, M., Young, G.T., Zwart, R., Sher, E., Millar, N.S., 2011. Agonist activation of α7 nicotinic acetylcholine receptors via an allosteric transmembrane site. Proc. Natl. Acad. Sci. U.S.A. 108, 5867–5872. https://doi.org/10.1073/pnas.1017975108.

Grazioso, G., Cavalli, A., De Amici, M., Recanatini, M., De Micheli, C., 2008. Alpha7 nicotinic acetylcholine receptor agonists: prediction of their binding affinity through a molecular mechanics Poisson-Boltzmann surface area approach. J. Comput. Chem. 29, 2593–2602. https://doi.org/10.1002/jcc.21019.

Grazioso, G., Pomè, D.Y., Matera, C., Frigerio, F., Pucci, L., Gotti, C., Dallanoce, C., Amici, M. De, 2009. Design of novel α7-subtype-preferring nicotinic acetylcholine receptor agonists: application of docking and MM-PBSA computational approaches, synthetic and pharmacological studies. Bioorg. Med. Chem. Lett 19, 6353–6357. https://doi.org/10.1016/j.bmcl.2009.09.073.

Grazioso, G., Sgrignani, J., Capelli, R., Matera, C., Dallanoce, C., De Amici, M., Cavalli, A., 2015. Allosteric modulation of alpha7 nicotinic receptors: mechanistic insight through metadynamics and essential dynamics. J. Chem. Inf. Model. 55, 2528–2539. https://doi.org/10.1021/acs.jcim.5b00459.

Grønlien, J.H., Håkerud, M., Ween, H., Thorin-Hagene, K., Briggs, C.A., Gopalakrishnan, M., Malysz, J., 2007. Distinct profiles of α7 nAChR positive allosteric modulation revealed by structurally diverse chemotypes. Mol. Pharmacol. 72, 715–724. https://doi.org/10.1124/mol.107.035410.

Grubmüller, H., Heymann, B., Tavan, P., 1996. Ligand binding: molecular mechanics calculation of the streptavidin-biotin rupture force (80-.). Science 271, 997. LP – 999.

Gulsevin, A., 2017. A Comparative Analysis of the Principles behind α7 Nicotinic Acetylcholine Receptor Function. University of Florida.

Gulsevin, A., Papke, R.L., Stokes, C., Garai, S., Thakur, G.A., Quadri, M., Horenstein, N. A., 2019. Allosteric agonism of α7 nicotinic acetylcholine receptors: receptor modulation outside the orthosteric site. Mol. Pharmacol. 95, 606–614. https://doi.org/10.1124/mol.119.115758.

Hamouda, A.K., Chiara, D.C., Sauls, D., Cohen, J.B., Blanton, M.P., 2006. Cholesterol interacts with transmembrane α-helices M1, M3, and M4 of the torpedo nicotinic acetylcholine receptor: photolabeling studies using [3H]azichoiesterol. Biochemistry 45, 976–986. https://doi.org/10.1021/bi051978h.

Hansen, S.B., Sulzenbacher, G., Huxford, T., Marchot, P., Taylor, P., Bourne, Y., 2005. Structures of Aplysia AChBP complexes with nicotinic agonists and antagonists reveal distinctive binding interfaces and conformations. EMBO J. 24, 3635–3646. https://doi.org/10.1038/sj.emboj.7600828.

Hassaine, G., Deluz, C., Grasso, L., Wyss, R., Tol, M.B., Hovius, R., Graff, A., Stahlberg, H., Tomizaki, T., Desmyter, A., Moreau, C., Li, X.-D., Poitevin, F., Vogel, H., Nury, H., 2014. X-ray structure of the mouse serotonin 5-HT_3 receptor. Nature 512, 276–281. https://doi.org/10.1038/nature13552.

Hénault, C.M., Sun, J., Therien, J.P.D., daCosta, C.J.B., Carswell, C.L., Labriola, J.M., Juranka, P.F., Baenziger, J.E., 2015. The role of the M4 lipid-sensor in the folding, trafficking, and allosteric modulation of nicotinic acetylcholine receptors. Neuropharmacology 96, 157–168. https://doi.org/10.1016/j.neuropharm.2014.11.011.

Henchman, R.H., Wang, H.-L., Sine, S.M., Taylor, P., McCammon, J.A., 2003. Asymmetric structural motions of the homomeric α7 nicotinic receptor ligand binding domain revealed by molecular dynamics simulation. Biophys. J. 85, 3007–3018. https://doi.org/10.1016/S0006-3495(03)74720-1.

Henchman, R.H., Wang, H.L., Sine, S.M., Taylor, P., McCammon, J.A., 2005. Ligand-induced conformational change in the α7 nicotinic receptor ligand binding domain. Biophys. J. 88, 2564–2576. https://doi.org/10.1529/biophysj.104.053934.

Hibbs, R.E., Gouaux, E., 2011. Principles of activation and permeation in an anion-selective Cys-loop receptor. Nature 474, 54–60. https://doi.org/10.1038/nature10139.

Horenstein, N.A., Papke, R.L., 2017. Anti-inflammatory silent agonists. ACS Med. Chem. Lett. 8, 10–12. https://doi.org/10.1021/acsmedchemlett.7b00368.

Horenstein, N.A., Papke, R.L., Kulkarni, A.R., Chaturbhuj, G.U., Stokes, C., Manther, K., Thakur, G.A., 2016. Critical molecular determinants of α7 nicotinic acetylcholine receptor allosteric activation: separation of direct allosteric activation and positive allosteric modulation. J. Biol. Chem. 291, 5049–5067. https://doi.org/10.1074/jbc.M115.692392.

Huang, X., Zheng, F., Chen, X., Crooks, P.A., Dwoskin, L.P., Zhan, C.G., 2006. Modeling subtype-selective agonists binding with α4β2 and α7 nicotinic acetylcholine receptors: effects of local binding and long-range electrostatic interactions. J. Med. Chem. 49, 7661–7674. https://doi.org/10.1021/jm0606701.

Huang, X., Zheng, F., Stokes, C., Papke, R.L., Zhan, C.G., 2008. Modeling binding modes of α7 nicotinic acetylcholine receptor with ligands: the roles of Gln117 and other residues of the receptor in agonist binding. J. Med. Chem. 51, 6293–6302. https://doi.org/10.1021/jm800607u.

Hucho, F., Oberthür, W., Lottspeich, F., 1986. The ion channel of the nicotinic acetylcholine receptor is formed by the homologous helices M II of the receptor subunits. FEBS Lett. 205, 137–142. https://doi.org/10.1016/0014-5793(86)80881-X.

Hung, A., Tai, K., Sansom, M.S.P., 2005. Molecular dynamics simulation of the M2 helices within the nicotinic acetylcholine receptor transmembrane domain: structure and collective motions. Biophys. J. 88, 3321–3333. https://doi.org/10.1529/biophysj.104.052878.

Hurst, R.S., Hajós, M., Raggenbass, M., Wall, T.M., Higdon, N.R., Lawson, J.A., Rutherford-Root, K.L., Berkenpas, M.B., Hoffmann, W.E., Piotrowski, D.W., Groppi, V.E., Allaman, G., Ogier, R., Bertrand, S., Bertrand, D., Arneric, S.P., 2005. A novel positive allosteric modulator of the α7 neuronal nicotinic acetylcholine receptor: *in vitro* and *in vivo* characterization. J. Neurosci. 25, 4396. LP – 4405.

Izrailev, S., Stepaniants, S., Balsera, M., Oono, Y., Schulten, K., 1997. Molecular dynamics study of unbinding of the avidin-biotin complex. Biophys. J. 72, 1568–1581. https://doi.org/10.1016/S0006-3495(97)78804-0.

Izrailev, S., Stepaniants, S., Isralewitz, B., Kosztin, D., Lu, H., Molnar, F., Wriggers, W., Schulten, K., 1999. Steered molecular dynamics. Comput. Mol. Dyn. Challenges, Methods, Ideas 4, 39–65. https://doi.org/10.1007/978-3-642-58360-5_2.

Kästner, J., 2011. Umbrella sampling. Wiley Interdiscip. Rev. Comput. Mol. Sci. 1, 932–942. https://doi.org/10.1002/wcms.66.

Kombo, D.C., Bencherif, M., 2013. Comparative study on the use of docking and Bayesian categorization to predict ligand binding to nicotinic acetylcholine receptors (nAChRs) subtypes. J. Chem. Inf. Model. 53, 3212–3222. https://doi.org/10.1021/ci400493a.

Kouvatsos, N., Giastas, P., Chroni-Tzartou, D., Poulopoulou, C., Tzartos, S.J., 2016. Crystal structure of a human neuronal nAChR extracellular domain in pentameric assembly: ligand-bound α2 homopentamer. Proc. Natl. Acad. Sci. U.S.A. 113, 9635–9640. https://doi.org/10.1073/pnas.1602619113.

Kuang, G., Wang, X., Halldin, C., Nordberg, A., Långström, B., Ågren, H., Tu, Y., 2016. Theoretical study of the binding profile of an allosteric modulator NS-1738 with a chimera structure of the α7 nicotinic acetylcholine receptor. Phys. Chem. Chem. Phys. 18, 28003–28009. https://doi.org/10.1039/C6CP02278B.

Labarca, C., Nowak, M.W., Zhang, H., Tang, L., Deshpande, P., Lester, H. a, 1995. Channel gating governed symmetrically by conserved leucine residues in the M2 domain of nicotinic receptors. Nature. https://doi.org/10.1038/376514a0.

Law, R.J., Henchman, R.H., McCammon, J.A., 2005. A gating mechanism proposed from a simulation of a human α7 nicotinic acetylcholine receptor. Proc. Natl. Acad. Sci. U.S.A. 102, 6813–6818. https://doi.org/10.1073/pnas.0407739102.

Lebbe, E.K.M., Peigneur, S., Wijesekara, I., Tytgat, J., 2014. Conotoxins Targeting nicotinic acetylcholine receptors: an overview. Mar. Drugs 12, 2970–3004. https://doi.org/10.3390/md12052970.

Leffler, A.E., Kuryatov, A., Zebroski, H.A., Powell, S.R., Filipenko, P., Hussein, A.K., Gorson, J., Heizmann, A., Lyskov, S., Tsien, R.W., Poget, S.F., Nicke, A., Lindstrom, J., Rudy, B., Bonneau, R., Holford, M., 2017. Discovery of peptide ligands through docking and virtual screening at nicotinic acetylcholine receptor homology models. Proc. Natl. Acad. Sci. U.S.A. 114, E8100–E8109. https://doi.org/10.1073/pnas.1703952114.

Levitt, M., Sander, C., Stern, P.S., 1985. Protein normal-mode dynamics: trypsin inhibitor, crambin, ribonuclease and lysozyme. J. Mol. Biol. 181, 423–447. https://doi.org/10.1016/0022-2836(85)90230-X.

Li, S.-X., Huang, S., Bren, N., Noridomi, K., Dellisanti, C.D., Sine, S.M., Chen, L., 2011. Ligand-binding domain of an α7-nicotinic receptor chimera and its complex with agonist. Nat. Neurosci. 14, 1253–1259.

Liu, X., Xu, Y., Li, H., Wang, X., Jiang, H., Barrantes, F.J., 2008. Mechanics of channel gating of the nicotinic acetylcholine receptor. PLoS Comput. Biol. 4 https://doi.org/10.1371/journal.pcbi.0040019, 0100–0110.

Lüdemann, S.K., Lounnas, V., Wade, R.C., 2000. How do substrates enter and products exit the buried active site of cytochrome P450cam? 2. Steered molecular dynamics and adiabatic mapping of substrate pathways. J. Mol. Biol. 303, 813–830. https://doi.org/10.1006/jmbi.2000.4155.

Lugovskoy, A.A., Maslennikov, I.V., Tchikin, L.D., Efremov, R.G., Ivanov, V.T., Arseniev, A.S., 1999. Spatial structure of the M2 transmembrane segment of the nicotinic acetylcholine receptor α-subunit. FEBS Lett. 457, 117–121. https://doi.org/10.1016/S0014-5793(99)01023-6.

Lyford, L.K., Sproul, A.D., Eddins, D., McLaughlin, J.T., Rosenberg, R.L., 2003. Agonist-induced conformational changes in the extracellular domain of α7 nicotinic acetylcholine receptors. Mol. Pharmacol. 64, 650–658. https://doi.org/10.1124/mol.64.3.650.

Ma, J., 2005. Usefulness and limitations of normal mode analysis in modeling dynamics of biomolecular complexes. Structure 13, 373–380. https://doi.org/10.1016/j.str.2005.02.002.

Malysz, J., Grønlien, J.H., Anderson, D.J., Håkerud, M., Thorin-Hagene, K., Ween, H., Wetterstrand, C., Briggs, C.A., Faghih, R., Bunnelle, W.H., Gopalakrishnan, M., 2009. In vitro pharmacological characterization of a novel allosteric modulator of α7 neuronal acetylcholine receptor, 4-(5-(4-chlorophenyl)-2-methyl-3- propionyl-1H-pyrrol-1-yl)benzenesulfonamide (A-867744), exhibiting unique pharmacological profile. J. Pharmacol. Exp. Therapeut. 330, 257–267. https://doi.org/10.1124/jpet.109.151886.

Martin, L.F., Freedman, R., 2007. Schizophrenia and the α7 nicotinic acetylcholine receptor. In: International Review of Neurobiology. Academic Press, pp. 225–246. https://doi.org/10.1016/S0074-7742(06)78008-4.

McLaughlin, J.T., Fu, J., Rosenberg, R.L., 2007. Agonist-driven conformational changes in the inner β-sheet of α7 nicotinic receptors. Mol. Pharmacol. 71, 1312. LP – 1318.

Miller, C., 1989. Genetic manipulation of ion channels: a new approach to structure and mechanism. Neuron 2, 1195–1205. https://doi.org/10.1016/0896-6273(89)90304-8.

Mineur, Y.S., Mose, T.N., Blakeman, S., Picciotto, M.R., 2017. Hippocampal α7 nicotinic ACh receptors contribute to modulation of depression-like behaviour in C57BL/6J mice. Br. J. Pharmacol. 1–12. https://doi.org/10.1111/bph.13769.

Miyazawa, A., Fujiyoshi, Y., Unwin, N., 2003. Structure and gating mechanism of the acetylcholine receptor pore. Nature 423, 949–955. https://doi.org/10.1038/nature01748.

Mnatsakanyan, N., Jansen, M., 2013. Experimental determination of the vertical alignment between the second and third transmembrane segments of muscle nicotinic acetylcholine receptors. J. Neurochem. 125, 843–854. https://doi.org/10.1111/jnc.12260.

Morales-Perez, C.L., Noviello, C.M., Hibbs, R.E., 2016. X-ray structure of the human α4β2 nicotinic receptor. Nature 538, 411–415. https://doi.org/10.1038/nature19785.

Mortier, J., Rakers, C., Bermudez, M., Murgueitio, M.S., Riniker, S., Wolber, G., 2015. The impact of molecular dynamics on drug design: applications for the characterization of ligand-macromolecule complexes. Drug Discov. Today 20, 686–702. https://doi.org/10.1016/j.drudis.2015.01.003.

Mowrey, D., Cheng, M.H., Liu, L.T., Willenbring, D., Lu, X., Wymore, T., Xu, Y., Tang, P., 2013. Asymmetric ligand binding facilitates conformational transitions in pentameric ligand-gated ion channels. J. Am. Chem. Soc. 135, 2172–2180. https://doi.org/10.1021/ja307275v.

Nasiripourdori, A., Taly, V., Grutter, T., Taly, A., 2011. From toxins targeting ligand gated ion channels to therapeutic molecules. Toxins (Basel) 3, 260–293. https://doi.org/10.3390/toxins3030260.

Nemecz, A., Taylor, P., 2011. Creating an α7 nicotinic acetylcholine recognition domain from the acetylcholine-binding protein: crystallographic and ligand selectivity analyses. J. Biol. Chem. 286, 42555–42565. https://doi.org/10.1074/jbc.M111.286583.

Newcombe, J., Chatzidaki, A., Sheppard, T.D., Topf, M., Millar, N.S., 2018. Diversity of nicotinic acetylcholine receptor positive allosteric modulators revealed by mutagenesis and a revised structural model. Mol. Pharmacol. 93, 128–140. https://doi.org/10.1124/mol.117.110551.

Nicke, A., Loughnan, M.L., Millard, E.L., Alewood, P.F., Adams, D.J., Daly, N.L., Craik, D. J., Lewis, R.J., 2003. Isolation, structure, and activity of GID, a novel α4/7-conotoxin with an extended N-terminal sequence. J. Biol. Chem. 278, 3137–3144. https://doi.org/10.1074/jbc.M210280200.

Noridomi, K., Watanabe, G., Hansen, M.N., Han, G.W., Chen, L., 2017. Structural insights into the molecular mechanisms of myasthenia gravis and their therapeutic implications. Elife 6, e23043. https://doi.org/10.7554/eLife.23043.

Palma, E., Bertrand, S., Binzoni, T., Bertrand, D., 1996. Neuronal nicotinic α7 receptor expressed in Xenopus oocytes presents five putative binding sites for methyllycaconitine. J. Physiol. 491, 151–161. https://doi.org/10.1113/jphysiol.1996.sp021203.

Palma, E., Maggi, L., Eusebi, F., Miledi, R., 1997. Neuronal nicotinic threonine-for-leucine 247 α7 mutant receptors show different gating kinetics when activated by acetylcholine or by the noncompetitive agonist 5-hydroxytryptamine. Proc. Natl. Acad. Sci. U.S.A. 94, 9915–9919. https://doi.org/10.1073/pnas.94.18.9915.

Papke, R.L., Horenstein, N.A., Kulkarni, A.R., Stokes, C., Corrie, L.W., Maeng, C.Y., Thakur, G.A., 2014. The activity of GAT107, an allosteric activator and positive modulator of α7 nicotinic acetylcholine receptors (nAChR), is regulated by aromatic amino acids that span the subunit interface. J. Biol. Chem. 289, 4515–4531. https://doi.org/10.1074/jbc.M113.524603.

Post-Munson, D.J., Pieschl, R.L., Molski, T.F., Graef, J.D., Hendricson, A.W., Knox, R.J., McDonald, I.M., Olson, R.E., Macor, J.E., Weed, M.R., Bristow, L.J., Kiss, L., Ahlijanian, M.K., Herrington, J., 2017. B-973, a novel piperazine positive allosteric modulator of the α7 nicotinic acetylcholine receptor. Eur. J. Pharmacol. 799, 16–25. https://doi.org/10.1016/j.ejphar.2017.01.037.

Purohit, P., Auerbach, A., 2013. Loop C and the mechanism of acetylcholine receptor-channel gating. J. Gen. Physiol. 141, 467–478. https://doi.org/10.1085/jgp.201210946.

Puskar, N.L., Xiu, X., Lester, H.A., Dougherty, D.A., 2011. Two neuronal nicotinic acetylcholine receptors, α4β4 and α7, show differential agonist binding modes. J. Biol. Chem. 286, 14618–14627. https://doi.org/10.1074/jbc.M110.206565.

Quadri, M., Garai, S., Thakur, G.A., Stokes, C., Gulsevin, A., Horenstein, N.A., Papke, R. L., 2019. Macroscopic and microscopic activation of α7 nicotinic acetylcholine receptors by the structurally unrelated allosteric agonist-positive allosteric modulators (ago-PAMs) B-973B and GAT107. Mol. Pharmacol. 95, 43–61. https://doi.org/10.1124/mol.118.113340.

Quadri, M., Papke, R.L., Horenstein, N.A., 2016. Dissection of *N,N*-diethyl-*N′*-phenylpiperazines as α7 nicotinic receptor silent agonists. Bioorg. Med. Chem. 24, 286–293. https://doi.org/10.1016/j.bmc.2015.12.017.

Quiram, P.A., Sine, S.M., 1998. Structural elements in α-conotoxin ImI essential for binding to neuronal α7 receptors. J. Biol. Chem. 273, 11007–11011.

Rahman, M., Teng, J., Worrell, B.T., Karlin, A., Stowell, M.H.B., Hibbs, R.E., Rahman, M., Teng, J., Worrell, B.T., Noviello, C.M., Lee, M., Karlin, A., 2020. Structure of the native muscle-type nicotinic receptor and inhibition by snake venom toxins article structure of the native muscle-type nicotinic receptor and inhibition by snake venom toxins. Neuron 1–11. https://doi.org/10.1016/j.neuron.2020.03.012.

Revah, F., Bertrand, D., Galzi, J.L., Devillers-Thiéry, A., Mulle, C., Hussy, N., Bertrand, S., Ballivet, M., Changeux, J.P., 1991. Mutations in the channel domain alter desensitization of a neuronal nicotinic receptor. Nature 353, 846–849. https://doi.org/10.1038/353846a0.

Samson, A.O., Levitt, M., 2008. Inhibition mechanism of the acetylcholine receptor by α-neurotoxins as revealed by normal-mode dynamics. Biochemistry 47, 4065–4070. https://doi.org/10.1021/bi702272j.

Sankararamakrishnan, R., Adcock, C., Sansom, M.S., 1996. The pore domain of the nicotinic acetylcholine receptor: molecular modeling, pore dimensions, and electrostatics. Biophys. J. 71, 1659–1671. https://doi.org/10.1016/S0006-3495(96)79370-0.

Sansom, M.S.P., Sankararamakrishnan, R., Kerr, I.D., 1995. Modelling membrane proteins using structural restraints. Nat. Struct. Biol. 2, 624–631.

Schlitter, J., Engels, M., Krüger, P., Jacoby, E., Wollmer, A., 1993. Targeted molecular dynamics simulation of conformational change - application to the T ↔ R transition in insulin. Mol. Simulat. 10, 291–308. https://doi.org/10.1080/08927029308022170.

Schmitt, J.D., Sharples, C.G.V., Caldwell, W.S., 1999. Molecular recognition in nicotinic acetylcholine receptors: the importance of π-cation interactions. J. Med. Chem. 42, 3066–3074. https://doi.org/10.1021/jm990093z.

Schymkowitz, J., Borg, J., Stricher, F., Nys, R., Rousseau, F., Serrano, L., 2005. The FoldX web server: an online force field. Nucleic Acids Res. 33, W382–W388. https://doi.org/10.1093/nar/gki387.

Séguéla, P., Wadiche, J., Dineley-Miller, K., Dani, J.A., Patrick, J.W., 1993. Molecular cloning, functional properties, and distribution of rat brain α7: a nicotinic cation channel highly permeable to calcium. J. Neurosci. 13, 596–604.

Shahsavar, A., Gajhede, M., Kastrup, J.S., Balle, T., 2015. Structural studies of nicotinic acetylcholine receptors: using acetylcholine-binding protein as a structural

surrogate. Basic Clin. Pharmacol. Toxicol. 118, 399–407. https://doi.org/10.1111/bcpt.12528.
Sixma, T.K., Smit, A.B., 2003. Acetylcholine binding protein (AChBP): a secreted glial protein that provides a high-resolution model for the extracellular domain of pentameric ligand-gated ion channels. Annu. Rev. Biophys. Biomol. Struct. 32, 311–334. https://doi.org/10.1146/annurev.biophys.32.110601.142536.
Smit, A.B., Syed, N.I., Schaap, D., van Minnen, J., Klumperman, J., Kits, K.S., Lodder, H., van der Schors, R.C., van Elk, R., Sorgedrager, B., Brejc, K., Sixma, T.K., Geraerts, W. P.M., 2001. A glia-derived acetylcholine-binding protein that modulates synaptic transmission. Nature 411, 261–268.
Spurny, R., Debaveye, S., Farinha, A., Veys, K., Vos, A.M., Gossas, T., Atack, J., Bertrand, S., Bertrand, D., Danielson, U.H., Tresadern, G., Ulens, C., 2015. Molecular blueprint of allosteric binding sites in a homologue of the agonist-binding domain of the α7 nicotinic acetylcholine receptor. Proc. Natl. Acad. Sci. U.S.A. 112, E2543–E2552. https://doi.org/10.1073/pnas.1418289112.
Stokes, C., Treinin, M., Papke, R.L., 2015. Looking below the surface of nicotinic acetylcholine receptors. Trends Pharmacol. Sci. 36, 514–523. https://doi.org/10.1016/j.tips.2015.05.002.
Suresh, A., Hung, A., 2019. Structural effects of divalent calcium cations on the α7 nicotinic acetylcholine receptor: a molecular dynamics simulation study. Proteins Struct. Funct. Bioinf. 1–14. https://doi.org/10.1002/prot.25761.
Suresh, A., Hung, A., 2016. Molecular simulation study of the unbinding of α-conotoxin [γ4E]GID at the α7 and α4β2 neuronal nicotinic acetylcholine receptors. J. Mol. Graph. Model. 70, 109–121. https://doi.org/10.1016/j.jmgm.2016.09.006.
Tabassum, N., Ma, Q., Wu, G., Jiang, T., Yu, R., 2017. Exploring the binding energy profiles of full agonists, partial agonists, and antagonists of the α7 nicotinic acetylcholine receptor. J. Mol. Model. 23, 251. https://doi.org/10.1007/s00894-017-3419-4.
Tamamizu, S., Guzmán, G.R., Santiago, J., Rojas, L.V., McNamee, M.G., Lasalde-Dominicci, J.A., 2000. Functional effects of periodic tryptophan substitutions in the α M4 transmembrane domain of the Torpedo californica nicotinic acetylcholine receptor. Biochemistry 39, 4666–4673. https://doi.org/10.1021/bi992835w.
Targowska-Duda, K.M., Kaczor, A.A., Jozwiak, K., Arias, H.R., 2018. Molecular interactions of type I and type II positive allosteric modulators with the human α7 nicotinic acetylcholine receptor: an *in silico* study. J. Biomol. Struct. Dyn. 1102, 1–29. https://doi.org/10.1080/07391102.2018.1427634.
Thakur, G.A., Kulkarni, A.R., Deschamps, J.R., Papke, R.L., 2013. Expeditious synthesis, enantiomeric resolution, and enantiomer functional characterization of (4-(4-bromophenyl)-3a,4,5,9b-tetrahydro-3H-cyclopenta[c]quinoline-8-sulfonamide (4BP-TQS): an allosteric agonist-positive allosteric modulator of α7 nicotinic ac. J. Med. Chem. 56, 8943–8947. https://doi.org/10.1021/jm401267t.
Timmermann, D.B., Grønlien, J.H., Kohlhaas, K.L., Nielsen, E., Dam, E., Jørgensen, T.D., Ahring, P.K., Peters, D., Holst, D., Chrsitensen, J.K., Malysz, J., Briggs, C. a, Gopalakrishnan, M., Olsen, G.M., 2007. An allosteric modulator of the α7 nicotinic acetylcholine receptor possessing cognition-enhancing properties in vivo. J. Pharmacol. Exp. Therapeut. 323, 294–307. https://doi.org/10.1124/jpet.107.120436.vidual.
Torrie, G.M., Valleau, J.P., 1977. Nonphysical sampling distributions in Monte Carlo free-energy estimation: umbrella sampling. J. Comput. Phys. 23, 187–199. https://doi.org/10.1016/0021-9991(77)90121-8.
Ulens, C., Hogg, R.C., Celie, P.H., Bertrand, D., Tsetlin, V., Smit, A.B., Sixma, T.K., 2006. Structural determinants of selective α-conotoxin binding to a nicotinic acetylcholine receptor homolog AChBP. Proc. Natl. Acad. Sci. U.S.A. 103, 3615–3620. https://doi.org/10.1073/pnas.0507889103.
Unwin, N., 2005. Refined structure of the nicotinic acetylcholine receptor at 4 Å resolution. J. Mol. Biol. 346, 967–989. https://doi.org/10.1016/j.jmb.2004.12.031.
Unwin, N., 1995. Acetylcholine receptor channel imaged in the open state. Nature. https://doi.org/10.1038/373037a0.
Unwin, N., 1993. Nicotinic acetylcholine receptor an 9 Å resolution. J. Mol. Biol. https://doi.org/10.1006/jmbi.1993.1107.
Unwin, N., Fujiyoshi, Y., 2012. Gating movement of acetylcholine receptor caught by plunge-freezing. J. Mol. Biol. 422, 617–634. https://doi.org/10.1016/j.jmb.2012.07.010.
Van Arnam, E.B., Blythe, E.E., Lester, H.A., Dougherty, D.A., 2013. An unusual pattern of ligand-receptor interactions for the α7 nicotinic acetylcholine receptor, with implications for the binding of varenicline. Mol. Pharmacol. 84, 201–207. https://doi.org/10.1124/mol.113.085795.
Wallace, T.L., Ballard, T.M., Pouzet, B., Riedel, W.J., Wettstein, J.G., 2011. Drug targets for cognitive enhancement in neuropsychiatric disorders. Pharmacol. Biochem. Behav. https://doi.org/10.1016/j.pbb.2011.03.022.
Walsh, R.M., Roh, S.H., Gharpure, A., Morales-Perez, C.L., Teng, J., Hibbs, R.E., 2018. Structural principles of distinct assemblies of the human α4β2 nicotinic receptor. Nature 557, 261–265. https://doi.org/10.1038/s41586-018-0081-7.
Wang, Hong, Yu, M., Ochani, M., Amella, C.A., Tanovic, M., Susarla, S., Li, J.H., Wang, Haichao, Yang, H., Ulloa, L., Al-Abed, Y., Czura, C.J., Tracey, K.J., 2003. Nicotinic acetylcholine receptor α7 subunit is an essential regulator of inflammation. Nature 421, 384–388. https://doi.org/10.1038/nature01339.
Wells, S., Menor, S., Hespenheide, B., Thorpe, M.F., 2005. Constrained geometric simulation of diffusive motion in proteins. Phys. Biol. 2, S127–S136. https://doi.org/10.1088/1478-3975/2/4/S07.
Williams, D.K., Stokes, C., Horenstein, N.A., Papke, R.L., 2009. Differential regulation of receptor activation and agonist selectivity by highly conserved tryptophans in the nicotinic acetylcholine receptor binding site. J. Pharmacol. Exp. Therapeut. 330, 40–53. https://doi.org/10.1124/jpet.109.151225.
Williams, D.K., Wang, J., Papke, R.L., 2011. Investigation of the molecular mechanism of the α7 nicotinic acetylcholine receptor positive allosteric modulator PNU-120596 provides evidence for two distinct desensitized states. Mol. Pharmacol. 80, 1013. https://doi.org/10.1124/mol.111.074302. LP – 1032.
Xiao, Y., Hammond, P.S., Mazurov, A.A., Yohannes, D., 2012. Multiple interaction regions in the orthosteric ligand binding domain of the α7 neuronal nicotinic acetylcholine receptor. J. Chem. Inf. Model. 52, 3064–3073. https://doi.org/10.1021/ci3001953.
Xu, Y., Barrantes, F.J., Luo, X., Chen, K., Shen, J., Jiang, H., 2005. Conformational dynamics of the nicotinic acetylcholine receptor channel: a 35-ns molecular dynamics simulation study. J. Am. Chem. Soc. 127, 1291–1299. https://doi.org/10.1021/ja044577i.
Yamodo, I.H., Chiara, D.C., Cohen, J.B., Miller, K.W., 2010. Conformational changes in the nicotinic acetylcholine receptor during gating and desensitization. Biochemistry 49, 156–165. https://doi.org/10.1021/bi901550p.
Yi, M., Tjong, H., Zhou, H.-X., 2008. Spontaneous conformational change and toxin binding in α7 acetylcholine receptor: insight into channel activation and inhibition. Proc. Natl. Acad. Sci. U.S.A. 105, 8280–8285. https://doi.org/10.1073/pnas.0710530105.
Young, G.T., Zwart, R., Walker, A.S., Sher, E., Millar, N.S., 2008. Potentiation of α7 nicotinic acetylcholine receptors via an allosteric transmembrane site. Proc. Natl. Acad. Sci. U.S.A. 105, 14686–14691. https://doi.org/10.1073/pnas.0804372105.
Yu, C.R., Role, L.W., 1998. Functional contribution of the α7 subunit to multiple subtypes of nicotinic receptors in embryonic chick sympathetic neurones. J. Physiol. 509, 651–665. https://doi.org/10.1111/j.1469-7793.1998.651bm.x.
Yu, R., Craik, D.J., Kaas, Q., 2011. Blockade of neuronal α7-nAchR by α-Conotoxin ImI explained by computational scanning and energy calculations. PLoS Comput. Biol. 7 https://doi.org/10.1371/journal.pcbi.1002011.
Yu, R., Kaas, Q., Craik, D.J., 2012. Delineation of the unbinding pathway of α-conotoxin ImI from the α7 nicotinic acetylcholine receptor. J. Phys. Chem. B 116, 6097–6105. https://doi.org/10.1021/jp301352d.
Yu, R., Tae, H.S., Xu, Q., Craik, D.J., Adams, D.J., Jiang, T., Kaas, Q., 2019. Molecular dynamics simulations of dihydro-β-erythroidine bound to the human α4β2 nicotinic acetylcholine receptor. Br. J. Pharmacol. 176, 2750–2763. https://doi.org/10.1111/bph.14698.
Zhang, D., Gullingsrud, J., McCammon, J.A., 2006. Potentials of mean force for acetylcholine unbinding from the Alpha7 nicotinic acetylcholine receptor ligand-binding domain. J. Am. Chem. Soc. 128, 3019–3026. https://doi.org/10.1021/ja057292u.
Zhao, D., Xu, X., Pan, L., Zhu, W., Fu, X., Guo, L., Lu, Q., Wang, J., 2017. Pharmacologic activation of cholinergic alpha7 nicotinic receptors mitigates depressive-like behavior in a mouse model of chronic stress. J. Neuroinflammation 14, 234. https://doi.org/10.1186/s12974-017-1007-2.
Zhong, W., Gallivan, J.P., Zhang, Y., Li, L., Lester, H.A., Dougherty, D.A., 1998. From ab initio quantum mechanics to molecular neurobiology: a cation–π binding site in the nicotinic receptor. Proc. Natl. Acad. Sci. U.S.A. 95, 12088–12093. https://doi.org/10.1073/pnas.95.21.12088.
Zouridakis, M., Giastas, P., Zarkadas, E., Chroni-Tzartou, D., Bregestovski, P., Tzartos, S. J., 2014. Crystal structures of free and antagonist-bound states of human ± 9 nicotinic receptor extracellular domain. Nat. Struct. Mol. Biol. 21, 976–980. https://doi.org/10.1038/nsmb.2900.
Zouridakis, M., Papakyriakou, A., Ivanov, I.A., Kasheverov, I.E., Tsetlin, V., Tzartos, S., Giastas, P., 2019. Crystal structure of the monomeric extracellular domain of α9 nicotinic receptor subunit in complex with α-conotoxin RgIA: molecular dynamics insights into RgIA binding to α9α10 nicotinic receptors. Front. Pharmacol. 10, 474. https://doi.org/10.3389/fphar.2019.00474.
Zwart, R., Filippi, G. De, Broad, L.M., McPhie, G.I., Pearson, K.H., Baldwinson, T., Sher, E., De Filippi, G., Broad, L.M., McPhie, G.I., Pearson, K.H., Baldwinson, T., Sher, E., 2002. 5-Hydroxyindole potentiates human α7 nicotinic receptor-mediated responses and enhances acetylcholine-induced glutamate release in cerebellar slices. Neuropharmacology 43, 374–384. https://doi.org/10.1016/S0028-3908(02)00094-1.